Eosinophils protect against pulmonary hypertension through 14-HDHA and 17-HDHA

Ting Shu [1,5], Jiawei Zhang [1,5], Yitian Zhou [1,2], Zhihua Chen[3], Jinqiu Li[4], Qihao Tang[1], Wenqi Lei[1], Yanjiang Xing [4,6], Jing Wang [1,6] and Chen Wang[1,4]

[1]State Key Laboratory of Medical Molecular Biology, Haihe Laboratory of Cell Ecosystem, Dept of Pathophysiology, Institute of Basic Medical Sciences, Chinese Academy of Medical Sciences and Peking Union Medical College, Beijing, China. [2]MD Program, Peking Union Medical College, Beijing, China. [3]Key Laboratory of Respiratory Disease of Zhejiang Province, Dept of Respiratory and Critical Care Medicine, Second Affiliated Hospital of Zhejiang University School of Medicine, Hangzhou, Zhejiang, China. [4]State Key Laboratory of Medical Molecular Biology, Dept of Physiology, Institute of Basic Medical Sciences, Chinese Academy of Medical Sciences, Peking Union Medical College, Beijing, China. [5]These authors contributed equally to this manuscript. [6]J. Wang and Y. Xing contributed equally to this article as lead authors and supervised the work.

Corresponding author: Jing Wang (wangjing@ibms.pumc.edu.cn)

Shareable abstract (@ERSpublications)
EOS infiltrate lung tissues of PAH patients and PH mice. EOS deficiency aggravates PH development. EOS-derived 14-HDHA and 17-HDHA suppress inflammation through FPR2 and maintain pulmonary arterial smooth muscle cell homeostasis through PPARγ. https://bit.ly/3fjqGN3

Cite this article as: Shu T, Zhang J, Zhou Y, *et al*. Eosinophils protect against pulmonary hypertension through 14-HDHA and 17-HDHA. *Eur Respir J* 2023; 61: 2200582 [DOI: 10.1183/13993003.00582-2022].

Received: 17 March 2022
Accepted: 22 Oct 2022

Abstract

Background Pulmonary hypertension (PH) is a life-threatening disease featuring pulmonary vessel remodelling and perivascular inflammation. The effect, if any, of eosinophils (EOS) on the development of PH remains unclear.

Methods EOS infiltration and chemotaxis were investigated in peripheral blood and lung tissues from pulmonary arterial hypertension (PAH) patients without allergic history and from sugen/hypoxia-induced PH mice. The role of EOS deficiency in PH development was investigated using *GATA1*-deletion (ΔdblGATA) mice and anti-interleukin 5 antibody-treated mice and rats. Ultra-high-performance liquid chromatography-tandem mass spectrometry (UHPLC-MS/MS) was conducted to identify the critical oxylipin molecule(s) produced by EOS. Culture supernatants and lysates of EOS were collected to explore the mechanisms in co-culture cell experiments.

Results There was a lower percentage of EOS in peripheral blood but higher infiltration in lung tissues from PAH patients and PH mice. PAH/PH lungs showed increased EOS-related chemokine expression, mainly C-C motif chemokine ligand 11 derived from adventitial fibroblasts. EOS deficiency aggravated PH in rodents, accompanied by increased neutrophil and monocyte/macrophage infiltration. EOS highly expressed arachidonate 15-lipoxygenase (ALOX15). 14-hydroxy docosahexaenoic acid (14-HDHA) and 17-HDHA were critical downstream oxylipins produced by EOS, which showed anti-inflammatory effects on recruitment of neutrophils and monocytes/macrophages through N-formyl peptide receptor 2. They also repressed pulmonary artery smooth muscle cell (PASMC) proliferation by activating peroxisome proliferator-activated receptor γ and blunting Stat3 phosphorylation.

Conclusions In PH development without external stimuli, peripheral blood exhibits a low EOS level. EOS play a protective role by suppressing perivascular inflammation and maintaining PASMC homeostasis *via* 14/17-HDHA.

Introduction

Pulmonary arterial hypertension (PAH) is a severe life-threatening disease that features pulmonary vascular remodelling and perivascular inflammatory cell infiltration [1]. The enhanced T-helper 2 (Th2) cell immune response in PAH is well documented [2, 3]. However, the role of eosinophils (EOS), one of the Th2 effector cells [4], in PAH is seldom reported. A previous study showed that PAH patients with worse

syndromes had lower circulating EOS levels [5]; however, the functions of EOS in regulating PAH development and the detailed mechanisms remain unclear.

EOS are granulocytes with segmented nuclei and eosinophilic granules [6] that mature in bone marrow under a tightly regulated process directed by various transcription factors such as GATA1, GATA2 and FOG1 and cytokines such as interleukin 5 (IL5), and are then released into peripheral blood [7, 8]. Chemokines such as C-C motif chemokine ligand 11 (CCL11) (eotaxin-1), CCL24 (eotaxin-2) and CCL26 (eotaxin-3) and cytokines such as IL5 promote EOS transmigration into tissues [8, 9]. Once they have trafficked into tissues, EOS have a function in degranulation and cytokine release [10, 11], DNA release and eosinophil extracellular trap (EET) formation [12–14] and lipid metabolite production [6, 15, 16]. These processes facilitate the interaction of EOS with immune cells [15, 16] and tissue-resident cells [10, 11]. The detrimental roles of EOS have been widely recognised for decades, especially in asthma [4, 12]: EOS interact with mast cells [17], aid B-cells to produce antibodies [18, 19], promote Th2 polarisation [20] and mediate epithelial damage [4, 21]. However, EOS have regained attention in recent years because they show protective effects in maintaining tissue homeostasis in heart [11], lung [15], liver [22], gut [16] and adipose tissue [23, 24], which suggests that EOS have distinct roles in physiology and pathophysiology processes.

To determine the effect, if any, of EOS on PAH development, we explored the function and underlying mechanisms of action of lung EOS in PAH patients and in the sugen/hypoxia (SuHx)-induced PH rat or mouse model. We found that EOS migrated from peripheral blood to lung tissues in PAH patients and PH mice. By using *GATA1*-deletion (ΔdblGATA) mice and anti-IL5 antibody (TRFK5)-treated mice and rats, we found EOS deficiency worsened PH development by aggravating perivascular inflammation and pulmonary artery smooth muscle cell (PASMC) proliferation in animal models. Finally, we show that EOS function by releasing lipid mediators, among which 14-hydroxy docosahexaenoic acid (14-HDHA) and 17-hydroxy docosahexaenoic acid (17-HDHA) exert a protective effect in PH.

Methods

Human subjects

From 2016 to 2018, we enrolled 123 patients with either idiopathic PAH (IPAH) or heritable PAH (HPAH) and 119 healthy controls who were sex- and age-matched into our single-centre clinical study in Fuwai Hospital, Beijing. Patients with IPAH/HPAH had been diagnosed using the 2015 European Society of Cardiology/European Respiratory Society guidelines [25], and these diagnoses were also compatible with the IPAH/HPAH criteria described in the 6th World Symposium on Pulmonary Hypertension [26]. We excluded patients who were found to have 1) allergy, infection or autoimmune diseases; 2) tumours or fibrosis; or 3) age <18 years. Potential subjects were screened with a patient health questionnaire to establish their medical history. In the healthy control group, subjects with no history of PH, cardiovascular diseases, pulmonary diseases, cancer, infection, allergy or autoimmune diseases were included, and patients with an abnormal body mass index or aberrant routine blood work results were excluded. Lung tissue samples from five PAH patients were obtained through the China-Japan Friendship Hospital Lung Transplantation Center between 2018 and 2019. Lung tissue specimens found to have lung infection, allergic diseases or autoimmune diseases or complicated pulmonary diseases (*e.g.* tumours, fibrotic regions) were excluded. For our control group, five non-PAH lung tissue samples originating from healthy transplant donors were collected. Enrolled subjects gave informed consent to participate in this study. Approval for this study was provided by the Institutional Ethics Committee of Peking Union Medical College (2018043) and Fuwai Hospital (approval number 2017-877).

Animal models

ΔdblGATA mice were purchased from Jackson Laboratory (033551). Male hemizygote mice (ΔdblGATA/Y) and female heterozygote mice (ΔdblGATA/+) were maintained in a C57BL/6 genetic background to generate wild-type (WT) (+/Y) and knockout (KO) (ΔdblGATA/Y) littermates. C57BL/6 mice and Sprague Dawley rats were purchased from Beijing Vital River Laboratory Animal Technology Co., Ltd. Animals were randomly assigned to various treatment groups for each experiment. Mice or rats were maintained on a 12-h light–dark cycle with a regular unrestricted diet. To establish a SuHx-induced PH mouse model, 8–10-week-old male or female mice received weekly subcutaneous injections of SU5416 (20 $mg \cdot kg^{-1}$; S8442, Sigma Aldrich) for 3 weeks and were housed in an airtight plexiglass chamber (China Innovation Instrument) with 10% O_2 [27]. To establish a SuHx-induced PH rat model, 200 g male rats received a single SU5416 injection (20 $mg \cdot kg^{-1}$) and were then housed in 10% O_2 for 3 weeks. For the EOS depletion mouse model, the anti-IL5-neutralising antibody TRFK5 (554391, BD Pharmingen) was administrated at a dose of 2 µg per mouse each week, with a total of three doses for each mouse, through intravenous injection [28]. Sex- and age-matched littermates injected with an equal dose of isotype control

antibody (IgG1κ; 559072, BD Pharmingen) were used as controls. For the EOS-depletion rat model, the anti-IL5-neutralising antibody TRFK5 (14-7052-85, Invitrogen) was administrated at a dose of 17.5 μg per rat each week, three doses for each rat, and isotype control antibody was injected at an equal volume. For N-formyl peptide receptor 2 (FPR2) agonist Ac2-26 (HY-P1098A, MCE) treatment, mice were intraperitoneally injected at a dose of 50 μg per mouse every 3 days. The control mice were injected with an equal volume of vehicle. All animal experiments were conducted under the approval of the Animal Research Committee of the Institute of Laboratory Animals, Chinese Academy of Medical Sciences, and Peking Union Medical College (ACUC-A01-2020-017).

Additional materials and methods are available in the supplementary material.

Results

EOS populations decrease in blood while lung infiltration increases in PAH patients

To examine changes in EOS abundance during PAH progression, we enrolled 123 IPAH/HPAH patients and 119 age-/sex-matched healthy control subjects (supplementary table S1). Quantification of EOS by routine tests in peripheral blood samples indicated that the EOS percentage in PAH patients was significantly lower than that in sex-matched healthy control subjects (figure 1a). Further classification of PAH patients according to the New York Heart Association revealed that type I/II patients had a higher proportion of EOS in peripheral blood compared with type III/IV patients (figure 1b). These observations were both consistent with previous reports [5]. Notably, loss-of-function mutations of bone morphogenetic protein receptor 2 (*BMPR2*) are found in IPAH/HPAH, and patients who carry a causative mutation in *BMPR2* show more severe vascular dysfunction [29]. Here, we found that carriers of the *BMPR2* mutation also had a lower percentage of EOS in peripheral blood than non-carriers (figure 1c). To further examine changes in the abundance of EOS in lung tissues associated with PAH, we conducted EOS staining assays of lung tissue samples from PAH and non-PAH subjects. Hematoxylin and eosin (H&E) staining indicated enhanced EOS infiltration into PAH lung tissues, characterised by the accumulation of red-staining granulocytes with segmented nuclei around remodelled pulmonary vessels (figure 1d). Immunohistochemistry staining showed that eosinophil cationic protein $(ECP)^+$ EOS were more abundant in PAH lungs than in non-PAH lungs (figure 1d, e). Immunofluorescence staining also showed that most ECP^+ EOS were located closer to the $vimentin^+$ adventitial layer (figure 1f, arrow a). ECP^+ EOS were also found adhering to $CD31^+$ endothelial cells in the vascular lumen (figure 1f, arrow b). These observations suggest a dynamic process of EOS migration, with EOS recruited from the peripheral blood and residing in the parenchyma. In further support of this observed increase in EOS pulmonary migration, the expression of *IL5* and eotaxin genes (*CCL11*, *CCL24* and *CCL26*), which are necessary for EOS trafficking, was significantly elevated in PAH lung tissues (figure 1g), suggesting enhanced EOS recruitment in lungs during PAH development.

Taken together, these results indicate that EOS migrate to lung tissue during the progression of PAH in humans.

Decreased percentage of EOS in blood and increased proportions of EOS in lungs of PH mice

To determine whether these changes in EOS during PAH could also be observed in mice, we next established a SuHx-induced PH mouse model. We conducted flow cytometry analysis by staining for $CD45^+CD11b^+SiglecF^+$ EOS and found that the percentage of EOS in blood was significantly lower in PH mice than in control mice (figure 2a), while the percentage of EOS in PH lung tissue was significantly higher (figure 2b). EOS infiltration into the lungs was then confirmed by H&E and SiglecF staining (figure 2c). In addition, analyses of cytokine and chemokine expression indicated that both mRNA and protein expression of these markers was elevated in lung tissues of PH mice compared with controls (figure 2d, e). These findings were in agreement with our above results from PAH patients.

No significant changes were observed in EOS levels in either the bone marrow or spleen (figure 2f, g), suggesting that the production of EOS was unaffected during PH progression. However, EOS quantification showed a slight but significant increase in the percentage of EOS in remodelled right ventricle tissues (figure 2h), but no difference from controls in the left ventricle (figure 2i), suggesting that EOS may be related to impaired right ventricular function in PH. In lung tissues, EOS are classified as either resident eosinophils or inflammatory eosinophils based on CD101 expression [20]. Here we found that although there was a slight decrease in the percentage of $CD101^-$ resident EOS (from 91.2% to 85.4%) in PH lungs compared with controls (supplementary figure S1a), they were still the predominant subtype in lung and peripheral blood under PH (supplementary figure S1a, b) and the only detectable subtype in bone marrow of mice (supplementary figure S1c).

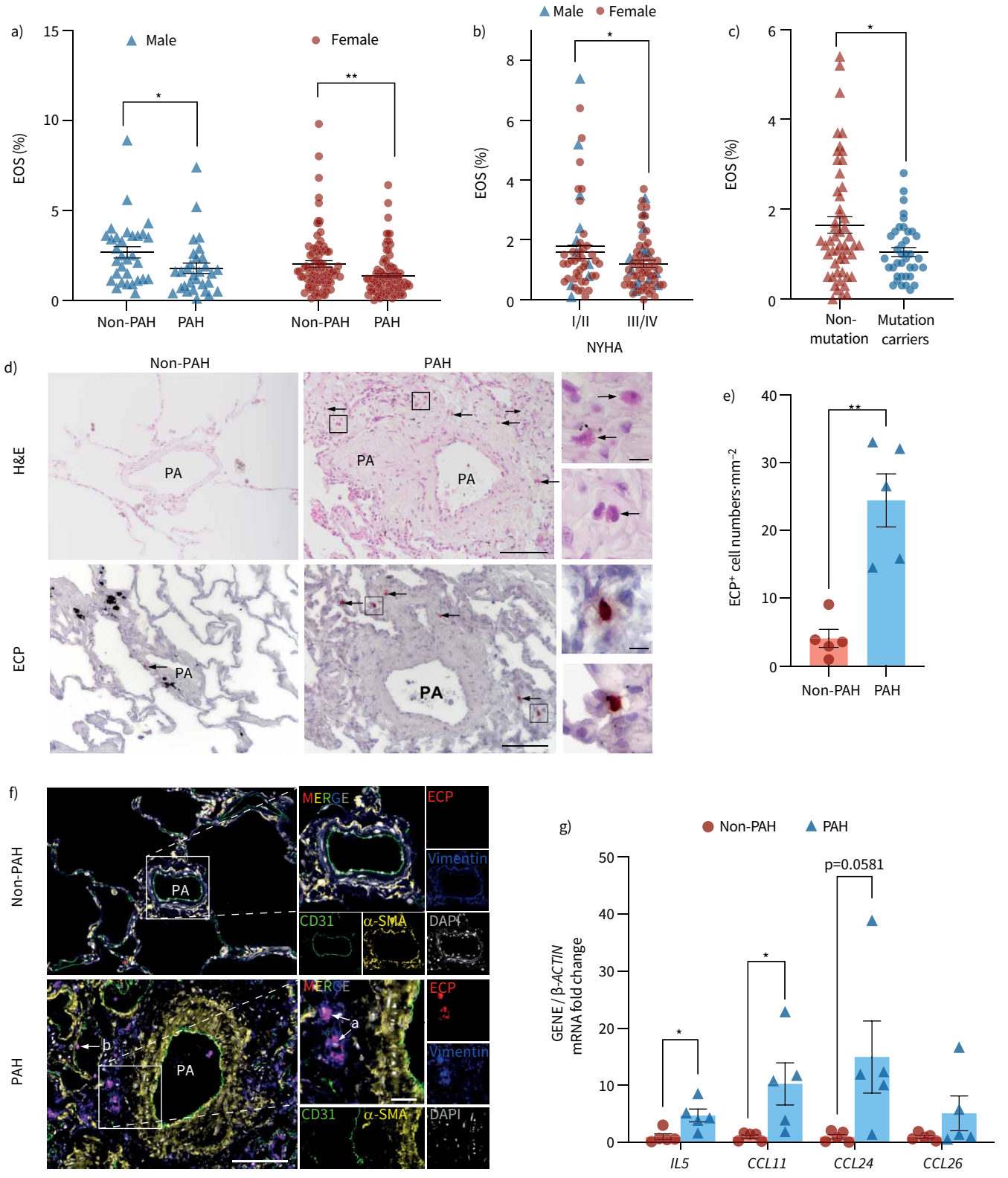

FIGURE 1 Increased lung eosinophil (EOS) accumulation in pulmonary arterial hypertension (PAH) patients. a) EOS percentage in blood of male/female PAH patients and sex-/age-matched healthy controls (male: non-PAH n=31, PAH n=30; female: non-PAH n=88, PAH n=93). b) EOS percentage in blood of PAH patients in New York Heart Association (NYHA) functional classes I/II and III/IV (I/II male:female ratio 16:39; III/IV male:female ratio 14:54). c) EOS percentage in blood of non-mutant and *BMPR2* mutation-carrying PAH patients (non-mutant n=52; mutation carrier n=38). d) Representative images of haematoxylin and eosin (H&E) and eosinophil cationic protein (ECP) immunohistochemical staining of

EOS (arrows) in lung sections from control subjects (non-PAH) or PAH patients. Scale bars: 100 μm (main) and 10 μm (inset). e) Quantification of ECP$^+$ cell numbers in lung sections from human samples (n=5 for each group). f) Representative images of CD31 (green), α-smooth muscle actin (α-SMA) (yellow), vimentin (blue) and ECP (red) immunofluorescent stainings of lung tissues from control subjects and PAH patients. Nuclei were counterstained with DAPI (white). EOS located close to vimentin$^+$ and CD31$^+$ areas are indicated by arrows a and b, respectively. Scale bars: 100 μm (main) and 25 μm (inset). g) Lung mRNA expression of *IL5*, *CCL11*, *CCL24* and *CCL26* (n=5 per group). All data are shown as mean±SEM. For a–c, e and g, differences were evaluated by unpaired two-tailed t-test. PA: pulmonary artery. *: p<0.05; **: p<0.01.

Collectively, these results show that the proportion of EOS decreases in blood but increases in lungs of PH mice, similar to what was observed in PAH patients.

CCL11 *upregulation in adventitial fibroblasts of PH lungs is associated with EOS recruitment*

In light of our observations of pulmonary EOS migration during PH, we next examined EOS trafficking-related cytokine and chemokine expression. Among all genes tested, *CCL11* (eotaxin-1) was the most highly expressed in mouse lungs (supplementary figure S2). Subsequent single-cell RNA sequencing (scRNA-seq) analysis of lung tissues from healthy humans (figure 3a) and control mice (figure 3b) revealed that a considerable proportion of fibroblasts expressed high levels of *CCL11* in both species.

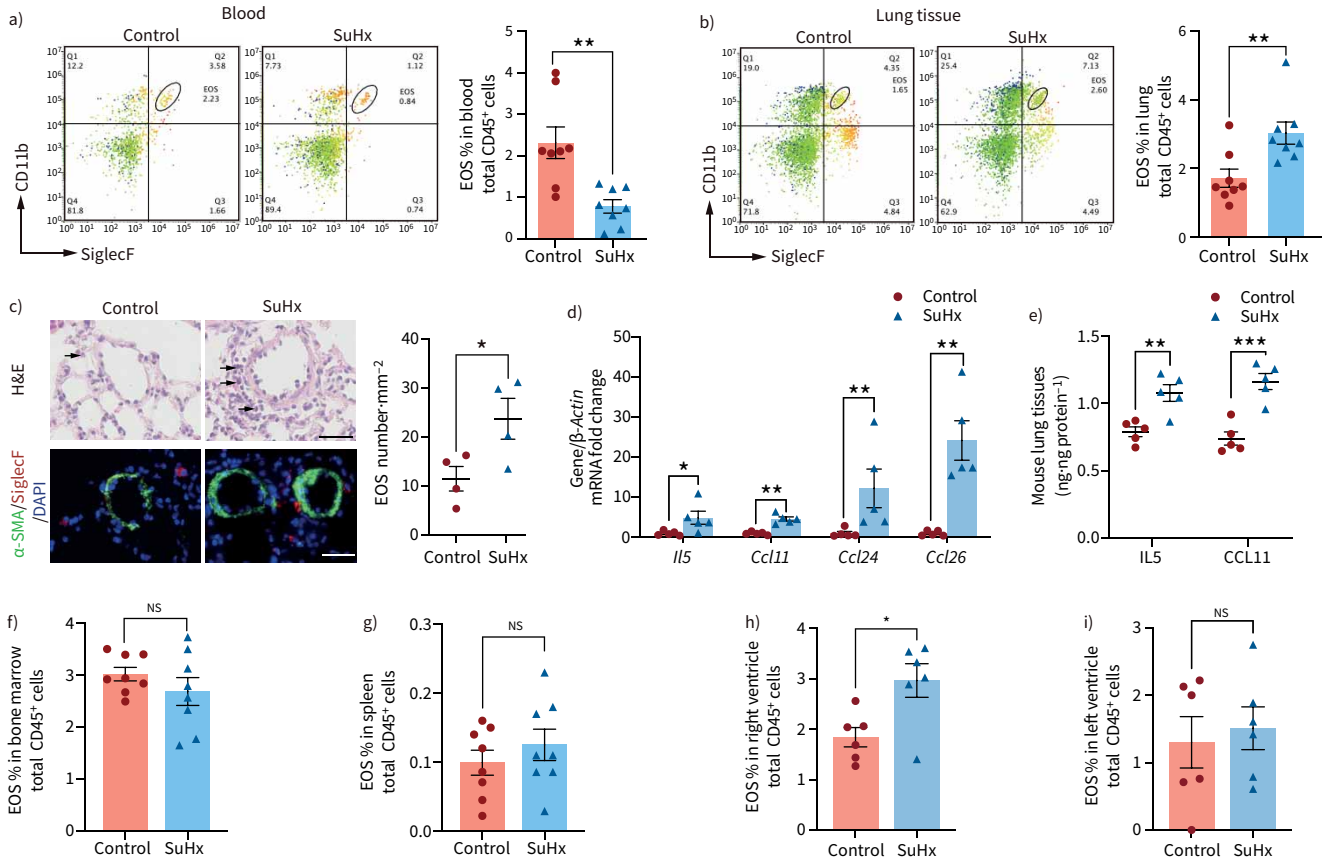

FIGURE 2 Increased lung eosinophil (EOS) accumulation in pulmonary hypertension (PH) mice. a) Flow cytometric analyses of CD11b$^+$SiglecF$^+$ EOS among CD45$^+$ cells in peripheral blood of control and sugen/hypoxia (SuHx)-induced PH mice. b) Flow cytometric analyses of CD11b$^+$SiglecF$^+$ EOS among CD45$^+$ cells in lung tissues of control and SuHx-induced PH mice (n=8 per group). c) Representative images of haematoxylin and eosin (H&E) and SiglecF immunofluorescent staining of EOS (arrows) in lung sections from control and SuHx-induced PH mice (left panel, scale bar: 25 μm) and quantification of EOS number in lung section (right panel, n=4 per group). d) Lung mRNA expression of *Il5*, *Ccl11*, *Ccl24* and *Ccl26* (n=5 per group). e) Lung IL5 and CCL11 protein levels in control or SuHx-induced PH mice (n=5 per group). f) The percentage of EOS among CD45$^+$ cells in bone marrow of control or SuHx-induced PH mice (n=8 per group). g) The percentage of EOS among CD45$^+$ cells in spleens of control or SuHx-induced PH mice (n=8 per group). h) The percentage of EOS among CD45$^+$ cells in right ventricles of control or SuHx-induced PH mice (n=6 per group). i) The percentage of EOS among CD45$^+$ cells in left ventricles of control or SuHx-induced PH mice (n=6 per group). All data are shown as mean±SEM. Differences were analysed by unpaired two-tailed t-test. NS: nonsignificant. *: p<0.05; **: p<0.01; ***: p<0.001.

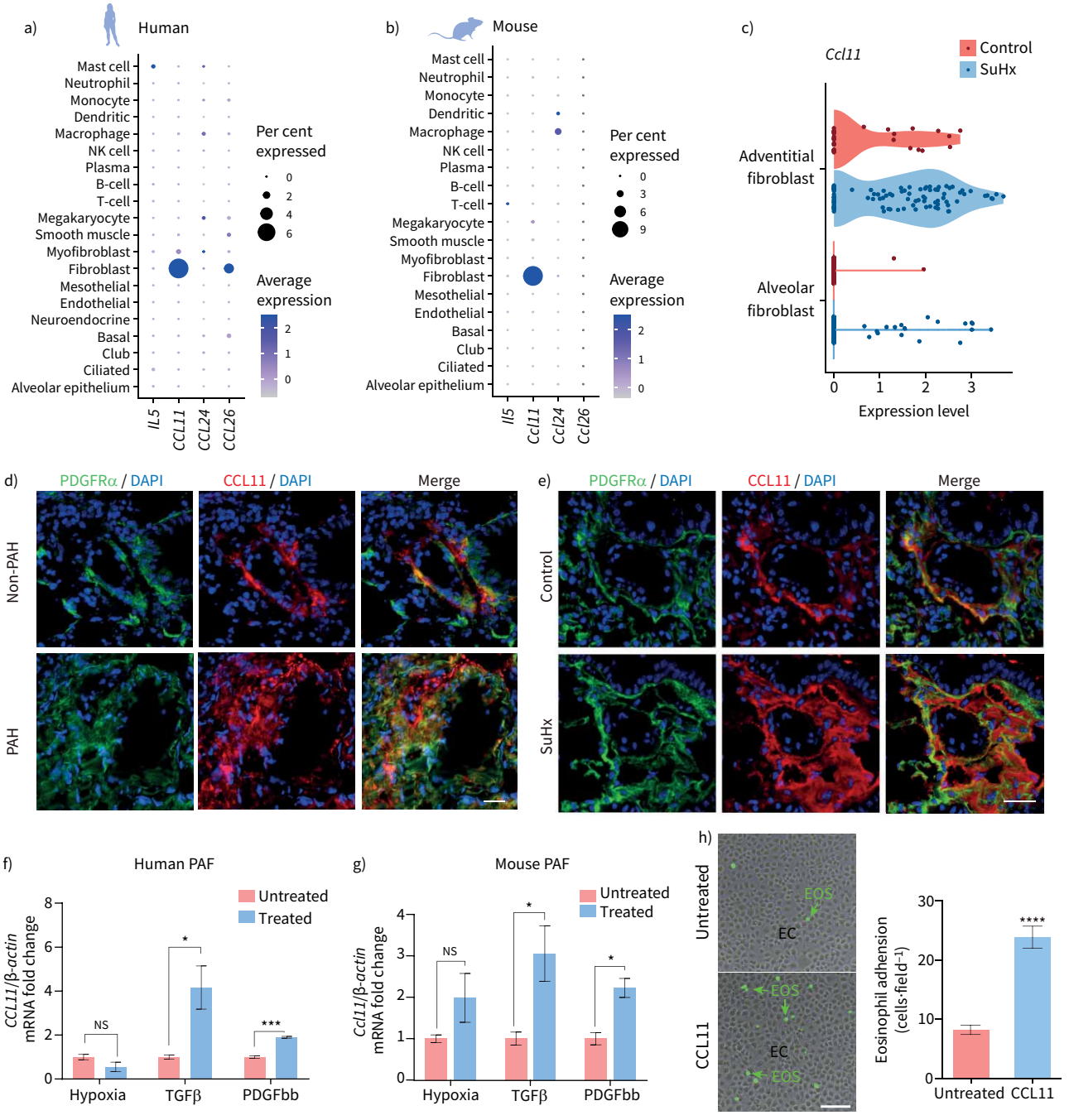

FIGURE 3 C-C motif chemokine ligand 11 (CCL11) expression in pulmonary adventitial fibroblasts. a) Dot plots of gene expression (*IL5*, *CCL11*, *CCL24* and *CCL26*) among cell clusters in human. b) Dot plots of gene expression (*Il5*, *Ccl11*, *Ccl24* and *Ccl26*) among cell clusters in mouse. c) Violin plots of the expression of *Ccl11* among two subgroups of fibroblasts in control and sugen/hypoxia (SuHx)-induced pulmonary hypertension (PH) mice lung tissue. d) Representative images of CCL11 and platelet-derived growth factor receptor α (PDGFRα) immunofluorescent staining of the lung sections from control subjects without pulmonary arterial hypertension (non-PAH) or PAH patients. Scale bar: 25 µm. e) Representative images of CCL11 and PDGFRα immunofluorescent staining of the lung sections from control or SuHx-induced PH mice. Scale bar: 25 µm. f) Relative mRNA expression of *CCL11* in human pulmonary adventitial fibroblasts (PAFs) under different treatments (n=3 for three independent repeats). g) Relative mRNA expression of *Ccl11* in mouse PAFs under different conditions (n=3 for three independent repeats). h) Representative images and quantification of eosinophil (EOS) adhesive assay. Green arrow points at the 5-(and 6)-carboxyfluorescein diacetate succinimidyl ester (CFSE)-labelled EOS (green). Scale bar: 100 µm. All data are shown as mean±SEM. Differences were evaluated by unpaired two-tailed t-test. NK: natural killer; TGFβ: transforming growth factor β; PDGFbb: platelet-derived growth factor bb; NS: nonsignificant. *: p<0.05; ***: p<0.001; ****: p<0.0001.

Further comparison of fibroblasts from PH mice showed that *Ccl11* was primarily expressed in adventitial rather than alveolar fibroblasts, and that both the percentage of cells and the average expression levels were greater in PH lung tissues than in control (figure 3c). Immunostaining of lung tissue from PAH patients and SuHx-induced PH mice showed that the area of tissue expressing CCL11 overlapped with that expressing platelet-derived growth factor receptor α (PDGFRα), which confirmed that CCL11 was derived from fibroblasts (figure 3d, e). However, CCL11 did not co-localise with CD31, α-smooth muscle actin (α-SMA), CD45 or club cell 10-kDa protein (CC10), which further suggests that endothelial cells, smooth muscle cells, immune cells and epithelial cells were not the main source of the CCL11 in lungs of PH mice (supplementary figure S3a–d). In human and mouse pulmonary adventitial fibroblasts activated by treatment with transforming growth factor β (TGFβ) or platelet-derived growth factor bb (PDGFbb), we found that *CCL11* expression was significantly higher than in untreated cells (figure 3f, g). Moreover, *CCL11* was not obviously upregulated in similarly treated endothelial cells or smooth muscle cells (supplementary figure S3e, f), allowing us to exclude these cell types as the main source of CCL11 during PH development. Using an EOS adhesion assay, we found that CCL11 stimulation increased EOS adhesion to endothelial cells (figure 3h), supporting the chemotaxis role of CCL11 in EOS recruitment. Collectively, these results suggest that the impaired function of pulmonary adventitial fibroblasts during PAH development results in enhanced CCL11 expression, which in turn promotes EOS migration.

EOS deficiency aggravates PH in animal models

To better understand the functional role of EOS in PH development, we induced PH in male EOS-deficient ΔdblGATA mice by exposing them to SuHx (figure 4a, supplementary figure S4). We first confirmed that the ΔdblGATA mice were deficient in EOS compared with WT mice (figure 4b, quantified in 4c). In addition, ΔdblGATA mice exhibited a significantly higher right ventricular systolic pressure and right ventricular hypertrophy index (weight of the right ventricle/left ventricle+septum (RV/LV+S)) than WT under PH (figure 4d, e), indicating that the deficiency of EOS further aggravated PH development. Immunostaining also showed that vascular thickening (figure 4f, quantified in 4g) and muscularisation (figure 4h) were more extensive in the absence of EOS in PH. Although fibroblasts were implicated in EOS recruitment (figure 3), no significant changes in pulmonary fibrosis were observed in EOS-deficient PH mouse lungs (supplementary figure S5a, b).

Because IL5 is crucial for EOS maturation and migration [8], depletion of EOS through IL5 neutralisation is applied clinically as a treatment for asthma [30]. Therefore, we depleted EOS by neutralising IL5 in C57BL/6 male mice. After injecting with anti-IL5 antibody (TRFK5), we induced PH in both TRFK5-treated male mice and isotype control-treated male mice (figure 4i). We found that the percentage of EOS was significantly lower in lung tissues of TRFK5-treated mice than in isotype control-treated mice (figure 4j, k). Furthermore, TRFK5 treatment resulted in a higher right ventricular systolic pressure and RV/LV+S in PH mice (figure 4l, m). Consistent with these observations, we also noted that vascular muscularisation was more extensive in EOS-depleted PH mice (figure 4n–p), without affecting pulmonary fibrosis (supplementary figure S5c, d). Because PAH is more predominant in females, we also examined the role of EOS in female mice by TRFK5 injection (supplementary figure S6a). Consistent with the observations in male mice, more severe PH phenotypes were observed in female SuHx-induced PH mice with EOS depletion than in isotype control-treated mice (supplementary figure S6b–g).

Because the rat PH model exhibited more severe progress than the mouse PH model, and shared more similarity with human PAH, we further explored the role of EOS in the SuHx-induced rat PH model. Male rats that received TRFK5 had a decreased blood EOS percentage (supplementary figure S7a, b) compared with the isotype control-treated mice. In the SuHx-induced rat PH model, EOS depletion resulted in more severe PH development and vascular muscularisation, which is consistent with observations in the mouse model (supplementary figure S7c–g).

Taken together, these results show that genetically or chemically induced EOS deficiency aggravates PH development, suggesting that EOS have a protective effect in PH development.

EOS deficiency leads to increased neutrophil and monocyte/macrophage infiltration during PH

We next sought to precisely define the effects of EOS in PH development. Because previous studies have shown that EOS participate in the regulation of immune homeostasis processes, such as Th2 polarisation [20], mast cell infiltration [17] and B-cell immunoglobulin production [18, 19], we examined how EOS deficiency affects different immune cell populations during PH in mice. Using flow cytometry-based assays to quantify the infiltration of different immune cells in ΔdblGATA mice, we observed no significant changes in the percentages of B-cells, T-cells (helper T-cells and cytotoxic T-cells), mast cells or dendritic cells compared with those in WT mice (supplementary figure S8a–e) under

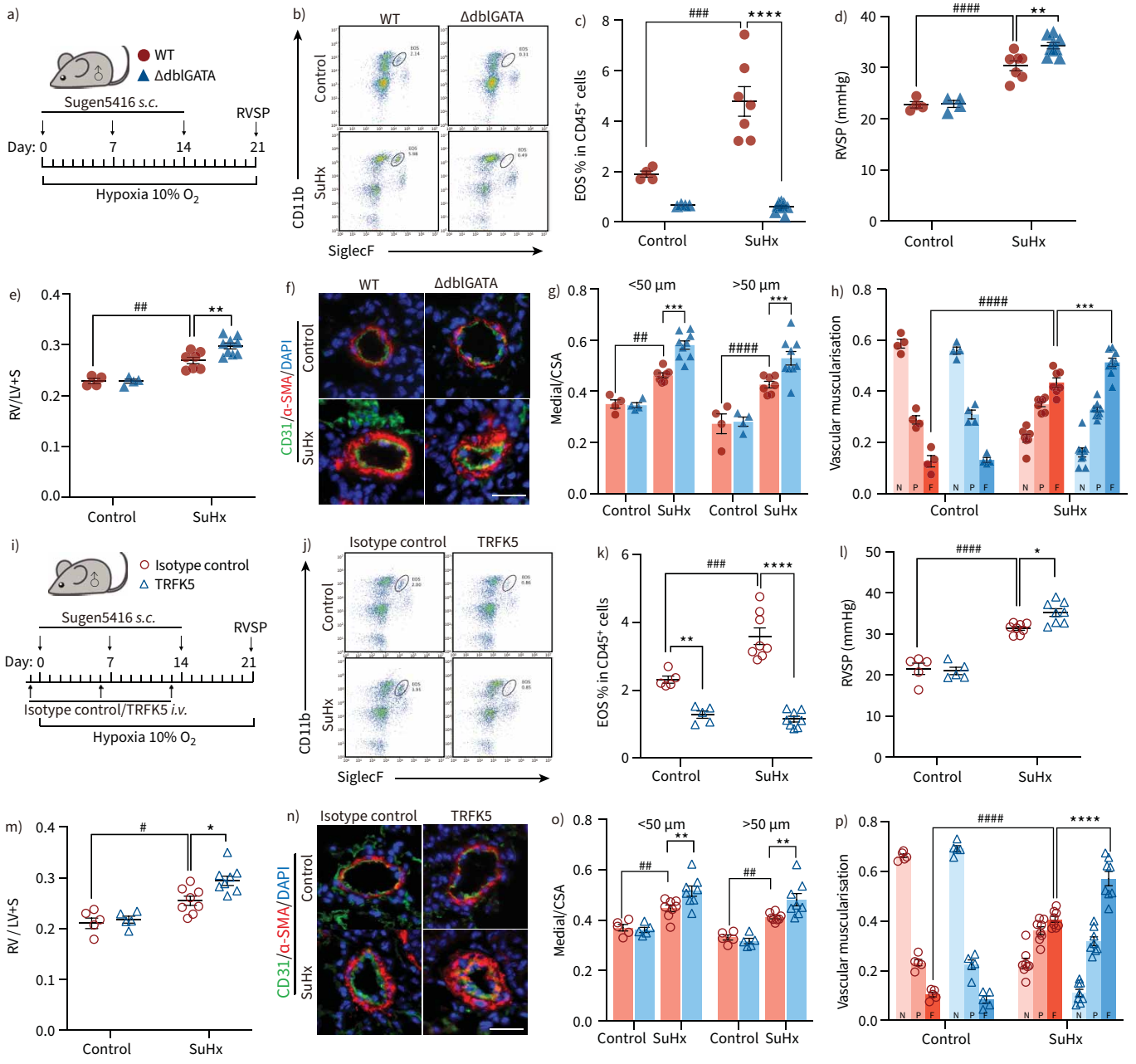

FIGURE 4 Eosinophil (EOS) deficiency and depletion exacerbate pulmonary hypertension (PH) in mice. a) Strategy for sugen/hypoxia (SuHx)-induced PH in wild-type (WT) or EOS-deficient (ΔdblGATA) male mice (control: n=4 per group; SuHx: n=7 for WT, n=9 for ΔdblGATA). b) Representative flow cytometric analyses of $CD11b^{+}SiglecF^{+}$ EOS among $CD45^{+}$ cells in lung tissues of WT or ΔdblGATA mice. c) The percentage of EOS among $CD45^{+}$ cells in lung tissues of WT or ΔdblGATA mice. d) Right ventricular systolic pressure (RVSP) of WT and ΔdblGATA mice. e) Right ventricular hypertrophy index (weight of the right ventricle/left ventricle+septum (RV/LV+S)) of the different experimental groups. f) Representative images of α-smooth muscle actin (α-SMA) and CD31 immunofluorescent staining of the lung sections from WT or ΔdblGATA mice. Scale bar: 25 μm. g) Quantification of pulmonary vascular medial thickness to total cross sectional area (CSA) for vessels of 20–50 μm and 50–100 μm in diameter. h) Proportion of vascular muscularisation of pulmonary vessels of 20–100 μm in diameter, classified as non-muscularised (N), partially muscularised (P) or fully muscularised (F). i) Strategy for SuHx-induced PH in male mice injected with isotype control antibody or TRFK5 (control: n=5 per group; SuHx: n=8 per group). j) Representative flow cytometric analyses of $CD11b^{+}SiglecF^{+}$ EOS among $CD45^{+}$ cells in lung tissues of isotype control- or TRFK5-treated mice. k) The percentage of EOS among $CD45^{+}$ cells in lung tissues of isotype control- or TRFK5-treated mice. l) RVSP of isotype control- or TRFK5-treated mice. m) Right ventricular hypertrophy of the different experimental groups. n) Representative images of α-SMA and CD31 immunofluorescent staining of the lung sections from isotype control- or TRFK5-treated mice. Scale bar: 25 μm. o) Quantification of wall thickness of the pulmonary vasculature for vessels of 20–50 μm and 50–100 μm in diameter. p) Proportion of vascular muscularisation of pulmonary vessels of 20–100 μm in diameter, classified as for g. All data are shown as mean±SEM. Differences between multiple groups were evaluated by two-way ANOVA with Bonferroni's *post hoc* test. *s.c.*: subcutaneous; *i.v.*: intravenous. *: p<0.05; **: p<0.01; ***: p<0.001; ****: p<0.0001 for ΔdblGATA *versus* WT mice or TRFK5- *versus* isotype control-treated mice. #: p<0.05; ##: p<0.01; ###: p<0.001; ####: p<0.0001 for mice in control *versus* SuHx groups.

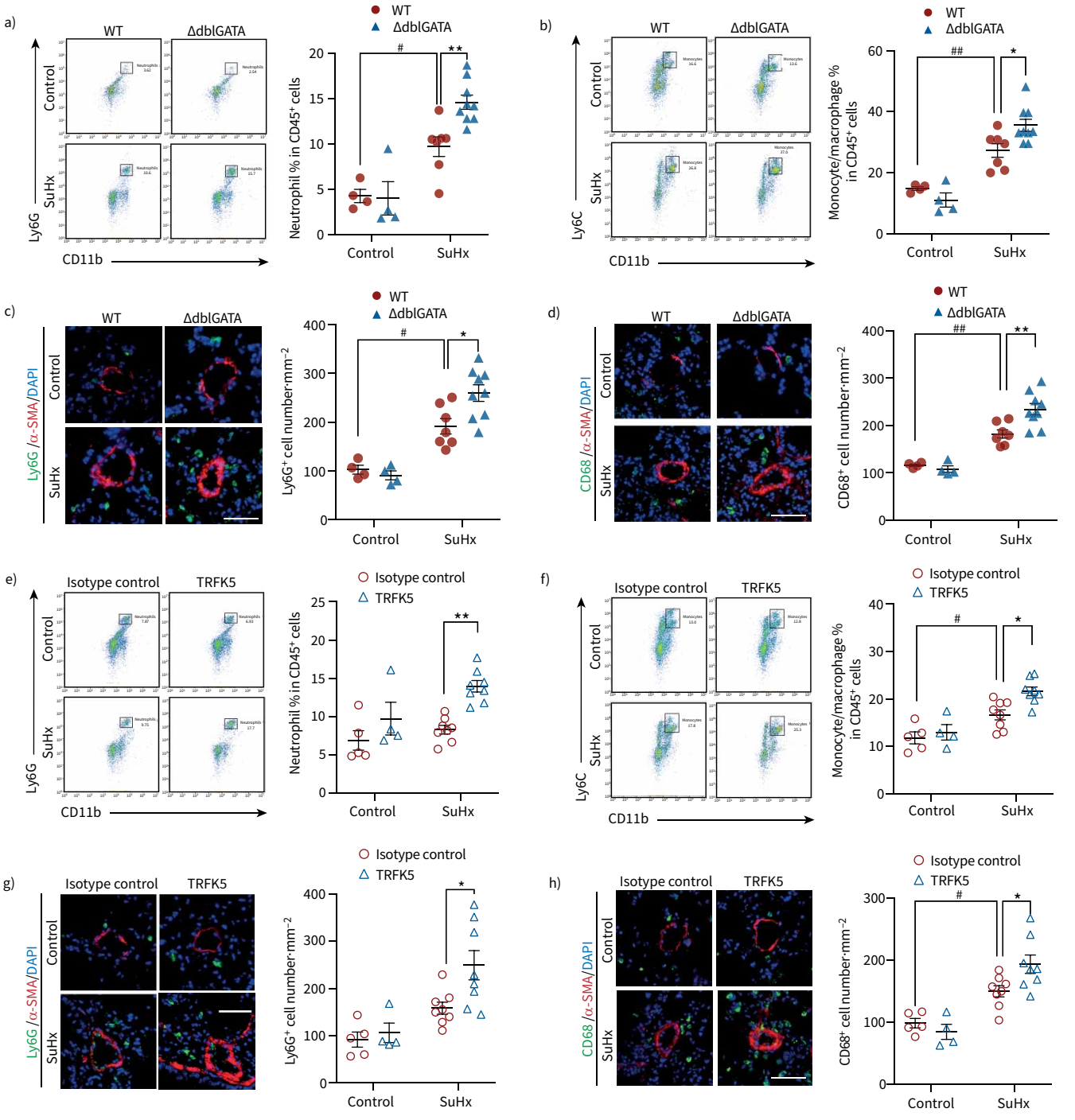

FIGURE 5 Eosinophil (EOS) deficiency or depletion promotes neutrophil and monocyte/macrophage accumulation in lung. a) Representative flow cytometric analyses of $CD11b^+Ly6G^+$ neutrophils among $CD45^+$ cells in lung tissues of wild-type (WT) or EOS-deficient (ΔdblGATA) male mice (left panel) and the percentage of neutrophils among $CD45^+$ cells (right panel). b) Representative flow cytometric analyses of $CD11b^+Ly6C^+$ monocytes/macrophages among $CD45^+$ cells in lung tissues of WT or ΔdblGATA male mice (left panel) and the percentage of monocytes/macrophages among $CD45^+$ cells (right panel). c) Representative images of Ly6G and α-smooth muscle actin (α-SMA) immunofluorescent staining of lung sections from WT or ΔdblGATA male mice (left panel) and quantification of $Ly6G^+$ cell numbers per mm^2 lung tissue (right panel). d) Representative images of CD68 and α-SMA immunofluorescent staining of lung sections from WT or ΔdblGATA male mice (left panel) and quantification of $CD68^+$ cell numbers per mm^2 lung tissue (right panel). e) Representative flow cytometric analyses of $CD11b^+Ly6G^+$ neutrophils among $CD45^+$ cells in lung tissues of isotype control- or TRFK5-treated male mice (left panel) and the percentage of neutrophils among $CD45^+$ cells (right panel). f) Representative flow cytometric analyses of $CD11b^+Ly6C^+$ monocytes/macrophages among $CD45^+$ cells in lung tissues of isotype control- or TRFK5-treated male mice (left panel) and the percentage of $CD11b^+Ly6C^+$ monocytes/macrophages among $CD45^+$ cells (right panel). g) Representative images of Ly6G and α-SMA immunofluorescent staining of lung sections from isotype control- or TRFK5-treated male mice (left

panel) and quantification of $Ly6G^+$ cell numbers per mm^2 lung tissue (right panel). h) Representative images of CD68 and α-SMA immunofluorescent staining of lung sections from isotype control- or TRFK5-treated male mice (left panel) and quantification of $CD68^+$ cell numbers per mm^2 lung tissue (right panel). Scale bars: 50 μm. Differences between multiple groups were evaluated by two-way ANOVA with Bonferroni's *post hoc* test. For a–d, control: n=4 per group; sugen/hypoxia (SuHx): n=7 for WT, n=9 for ΔdblGATA. For e–h, control: n=5 for isotype control, n=4 for TRFK5; SuHx: n=8 per group. All data are shown as mean±SEM. *: p<0.05; **: p<0.01 for ΔdblGATA *versus* WT mice, or TRFK5- *versus* isotype control-treated mice. #: p<0.05; ##: p<0.01 for mice in control *versus* SuHx groups.

PH. ELISA-based detection of immunoglobulin subtype levels indicated that EOS deficiency did not affect IgE, IgG or IgA production in lung tissues of PH mice (supplementary figure S8f–h).

Interestingly, we found increased proportions of $CD45^+CD11b^+Ly6G^+$ neutrophils and $CD45^+CD11b^+Ly6C^+$ monocytes/macrophages in lung tissues of EOS-deficient PH mice (figure 5a, b). Immunofluorescent staining further showed more $Ly6G^+$ neutrophils and $CD68^+$ monocytes/macrophages located around remodelled pulmonary vessels in lung tissues of EOS-deficient ΔdblGATA mice under PH (figure 5c, d). EOS depletion in TRFK5-treated mice also led to increased infiltration of neutrophils and monocytes/macrophages into lung tissues compared with that in the isotype control-treated mice with induced PH (figure 5e–h, supplementary figure S6h, i), without affecting other immune cell types (supplementary figure S9).

These observations of enhanced neutrophil and monocyte/macrophage infiltration indicate that EOS deficiency or depletion aggravates the PH-related inflammation of lung tissue in mice.

EOS suppress PASMC proliferation and migration

Increased pulmonary vascular muscularisation in ΔdblGATA mice during PH suggests a role for EOS in sustaining smooth muscle cells. To test this hypothesis, bone marrow-derived EOS were cultured, and the lysates and supernatants of harvested cells were used to treat PASMCs (figure 6a). After 14 days of culture, the percentage of $CD45^+CD11b^+SiglecF^+$ EOS in the total cell population reached 95% (figure 6b). PDGFbb-induced PASMC proliferation and migration were effectively suppressed by EOS lysates (figure 6c, d, quantified in 6g) and culture supernatants (figure 6e, f, quantified in 6h) in a dose-dependent manner. These observations suggest a beneficial role of EOS in regulating PASMC function.

14/17-HDHA contribute to the protective role of EOS in PH mice

Having revealed that EOS have anti-inflammatory and anti-proliferative effects in PH mice, we next sought to identify the essential underlying mechanism. One potential mechanism is the degranulation of EOS; however, we excluded this as a possibility because it seldom happens in mice [31]. Another mechanism is EET formation; however, there was no obvious EET formation in lungs of PH mice, as suggested by negative citrullinated histone H3 (H3Cit) staining (supplementary figure S10). Therefore, we hypothesised that lipid mediators released by EOS may play a critical role in exerting the protective effects. EOS contain polyunsaturated fatty acid oxidation enzymes, making them the major site of lipid metabolism [6]. To gain more insight into the pattern of lipid metabolism, EOS, $CD45^+$ cells (excluding EOS) and $CD45^-$ cells were sorted from lung cells of WT C57BL/6 mice by flow cytometry (figure 7a). By determining the mRNA expression of enzymes in the COX and LOX pathways, we found that gene expression for arachidonate 15-lipoxygenase (*Alox15*) was 90 times higher in EOS than in other immune cells and 160 times higher than in $CD45^-$ cells (figure 7a). Immunofluorescent staining showed that ALOX15 co-localised with $SiglecF^+$ cells in PH mouse lungs. No obvious $ALOX15^+$ staining was observed in the lung tissue of EOS-deficient ΔdblGATA mice (figure 7b). Western blot analysis also revealed significantly lower ALOX15 expression in ΔdblGATA mouse lungs (figure 7c) compared with WT lungs. Taken together, these results indicate that EOS are the main source of ALOX15.

Ultra-high-performance liquid chromatography-tandem mass spectrometry (UHPLC-MS/MS) was then performed on lung tissues from WT and ΔdblGATA PH mice to identify the specific lipid mediators derived from EOS (figure 7d, e). We found suppression of the 12/15-lipoxygenease pathway mediated by decreased ALOX15 expression in ΔdblGATA mouse lungs (figure 7f–h). The concentrations of downstream oxylipins were significantly lower in lung tissues from ΔdblGATA PH mice than in those from WT, including 12-HETE (17.38±2.28 $\mu g \cdot g^{-1}$ *versus* 8.25±1.30 $\mu g \cdot g^{-1}$), 14-HDHA (2.64±0.41 $\mu g \cdot g^{-1}$ *versus* 1.29±0.24 $\mu g \cdot g^{-1}$), 17-HDHA (0.28±0.04 $\mu g \cdot g^{-1}$ *versus* 0.09±0.01 $\mu g \cdot g^{-1}$) and 15-HEPE (0.05±0.01 $\mu g \cdot g^{-1}$ *versus* 0.03±0.01 $\mu g \cdot g^{-1}$) (figure 7f–h). These decreases suggest that oxylipins from the 12/15-lipoxygenease pathway are mainly derived from EOS.

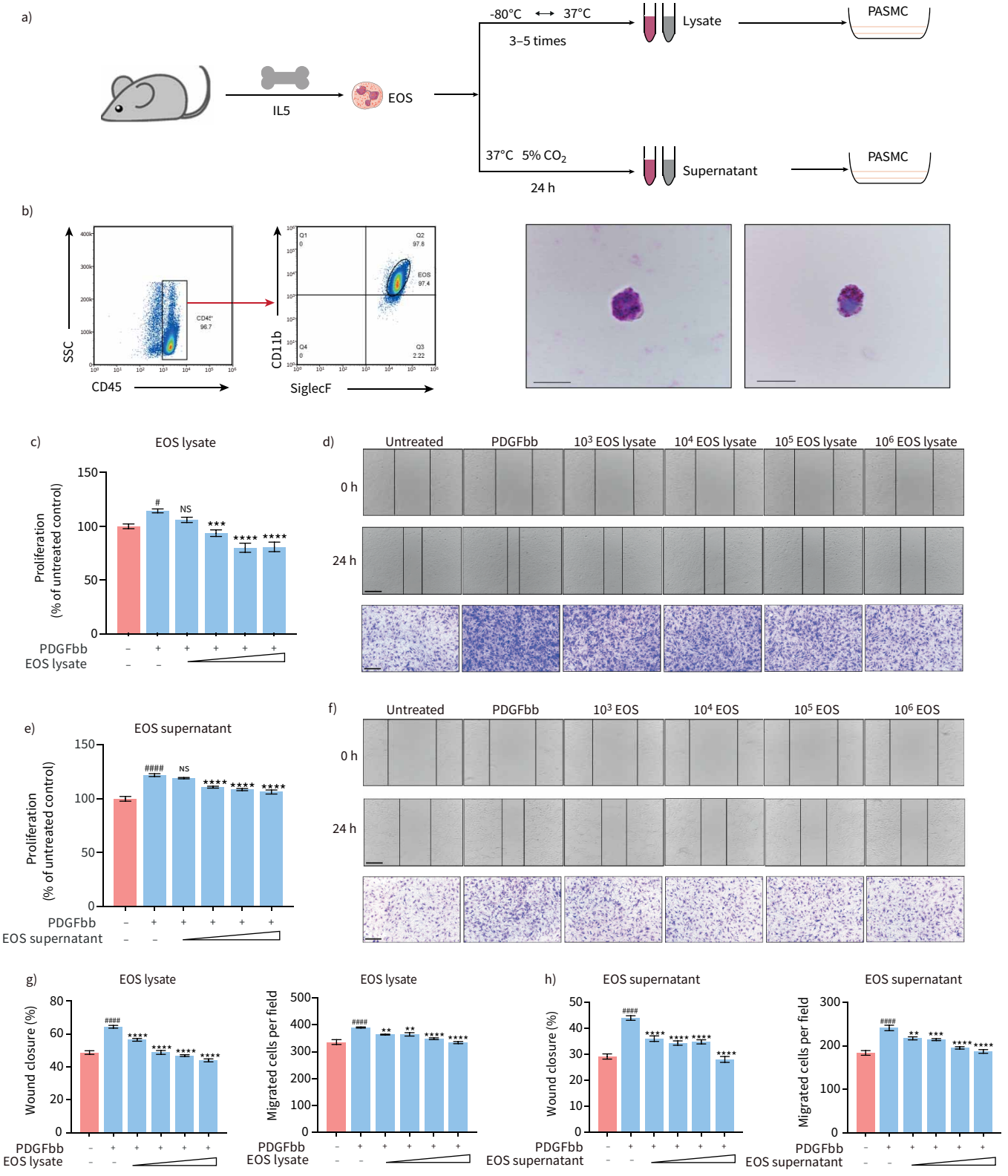

FIGURE 6 Eosinophils (EOS) abolish platelet-derived growth factor bb (PDGFbb)-induced smooth muscle cell proliferation and migration. a) Strategy for *in vitro* experiments. b) Representative flow cytometric identification (left panels) and Wright–Giemsa staining (right panels) of liquid-cultured bone marrow-derived EOS. Scale bars: 10 µm. c) The percentage of mouse pulmonary artery smooth muscle cell (PASMC) proliferation after 24-h treatment with PDGFbb (10 ng·mL^{-1}) and different concentrations of EOS lysate (equivalent to 1×10^3, 1×10^4, 1×10^5 and 1×10^6 EOS·mL^{-1}) compared with untreated control, measured by Cell Counting Kit-8 (Sigma Aldrich). d) Representative images of wound-healing

(upper panels) and Boyden chamber migration assay (bottom panel) for mouse PASMCs after 24-h treatment with PDGFbb (10 ng·mL^{-1}) and different concentrations of EOS lysate (equivalent to 1×10^3, 1×10^4, 1×10^5, 1×10^6 EOS·mL^{-1}). Scale bars: 250 μm. e) The percentage of mouse PASMC proliferation after 24-h treatment with PDGFbb (10 ng·mL^{-1}) and different concentrations of EOS supernatant (equivalent to 1×10^3, 1×10^4, 1×10^5, 1×10^6 EOS·mL^{-1}) compared with untreated control, measured by CCK8. f) Representative images of wound-healing (upper panels) and Boyden chamber migration assay (bottom panel) for mouse PASMCs after 24-h treatment with PDGFbb (10 ng·mL^{-1}) and different concentrations of EOS supernatant (equivalent to 1×10^3, 1×10^4, 1×10^5, 1×10^6 EOS·mL^{-1}). Scale bars: 250 μm. g) The percentage of wound closure (left panel) and quantification of migrated PASMCs (right panel) in d. h) The percentage of wound closure (left panel) and quantification of migrated PASMCs (right panel) in f. All data are shown as mean±SEM. Differences were evaluated by one-way ANOVA with Bonferroni's *post hoc* test. IL5: interleukin 5; SSC: side scatter; NS: nonsignificant. **: p<0.01; ***: p<0.001; ****: p<0.0001 for EOS lysate/supernatant-treated groups *versus* PDGFbb-treated groups. #: p<0.05; ####: p<0.0001 for PDGFbb-treated group compared with untreated control group.

To further validate the function of oxylipins, 14-HDHA, 17-HDHA, 15-HEPE and 12-HETE were chosen for *in vitro* PASMC proliferation assays (figure 7i). We found that 14-HDHA, 17-HDHA and 15-HEPE inhibited PDGFbb-induced proliferation in PASMCs at concentrations of 10 nM and 20 nM (figure 7i); these effects were consistent with those of EOS lysates and EOS supernatants (figure 6). Moreover, 14-HDHA and 17-HDHA are the precursors of specialised pro-resolving mediators (SPM) [32], and they exhibit pro-resolving functions through membrane receptors such as FPR2 [33, 34]. ScRNA-seq showed that FPR2 was mainly expressed in neutrophils, monocytes and macrophages (supplementary figure S11a, b), which was consistent with the observation that EOS deficiency promotes infiltration of neutrophils and monocytes/macrophages (figure 5). A leukocyte adhesion and transmigration assay showed that treatment with 14-HDHA and with 17-HDHA prevents neutrophil and monocyte/macrophage adhesion and migration. Pretreatment of neutrophils and monocytes/macrophages with the FPR2 inhibitor WRW4 blocked the effect caused by 14/17-HDHA (supplementary figure S11c–f). In EOS-deletion PH mice, FPR2 agonist Ac2-26 administration mitigated the pro-inflammatory effect caused by 14/17-HDHA shortage (supplementary figure S11g–i), suggesting the involvement of FPR2 in 14/17-HDHA-mediated anti-inflammatory effects.

Taken together, these results reveal that EOS exert anti-proliferative effects and anti-inflammatory effects *via* oxylipins such as 14/17-HDHA produced by 12/15-lipoxygenease.

14/17-HDHA suppress PASMC proliferation by activating PPARγ

The anti-inflammatory effects of 14-HDHA and 17-HDHA have been widely reported [32]. We further investigated the mechanism underlying the anti-proliferative effect of 14/17-HDHA. As previously reported, 12/15-lipoxygenase metabolites regulate lipid metabolism by activating peroxisome proliferator-activated receptor γ (PPARγ) [35], which is regarded as the major link between the TGFβ signalling and BMP2 signalling pathways during PAH development [36–38]. Once activated, PPARγ translocates into the nucleus and regulates downstream gene expression [36]. PPARγ activation also suppresses TGFβ-induced phosphorylation of Smad3 and Stat3 [36]. These events together repress the proliferation of smooth muscle cells. Therefore, we speculated that EOS regulates PASMC homeostasis through PPARγ and that 14/17-HDHA participates in this process. To test this, we first monitored PPARγ activation in PASMCs. PDGFbb treatment reduced PPARγ translocation into the nucleus (figure 8a, quantification in supplementary figure S12a) and enhanced Stat3 phosphorylation in PASMCs (figure 8b, quantification in supplementary figure S12b). Treatment with EOS supernatants reversed the effects induced by PDGFbb, as shown by increased PPARγ nuclear location and decreased Stat3 phosphorylation (figure 8a, b, supplementary figure S12a, b). By contrast, Smad3 phosphorylation did not decrease under EOS supernatant treatment, excluding the role of Smad3 signalling in this process (supplementary figure S13). GW9662, an irreversible PPARγ antagonist, abolished the anti-proliferative effect of EOS supernatant treatment (figure 8c). Also, downstream Stat3 phosphorylation increased when cells were treated with GW9662 (figure 8d, quantification in supplementary figure S12c). Having identified 14-HDHA and 17-HDHA as EOS-derived mediators that suppress PASMC proliferation (figure 7i), we then investigated whether 14/17-HDHA suppress PASMC proliferation through the PPARγ/Stat3 axis. PDGFbb-treated PASMCs were cultivated with 14-HDHA or 17-HDHA. We found that 14-HDHA and 17-HDHA treatment promoted PPARγ nuclear translocation and suppressed Stat3 phosphorylation (figure 8e, f, quantification in supplementary figure S12d, e).

These observations suggest that EOS, whose downstream lipid mediators 14-HDHA and 17-HDHA promote PPARγ nuclear translocation, sustain PASMC homeostasis through PPARγ/Stat3.

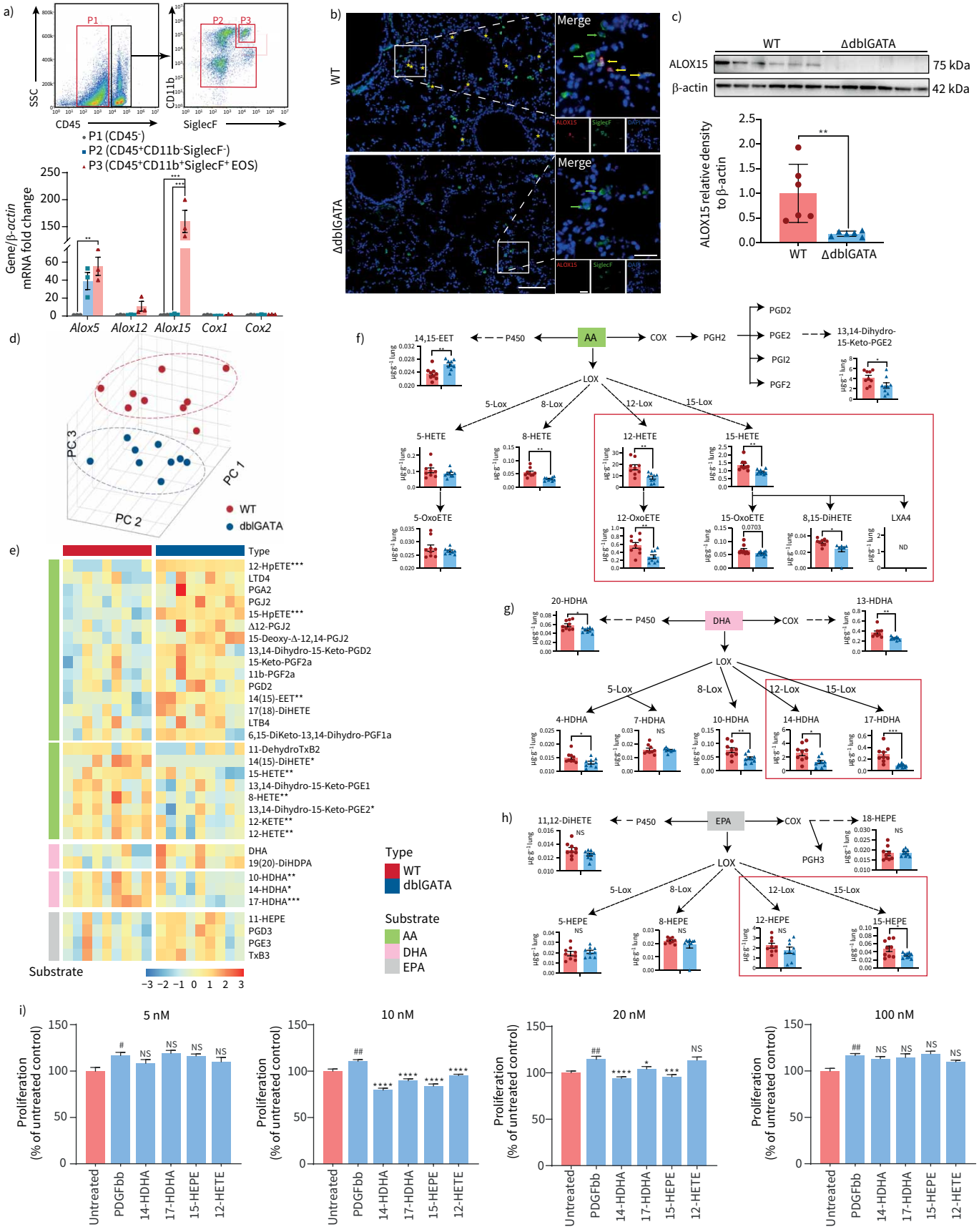
a)
P1
P2
P3
SSC
CD45
CD11b
SiglecF
P1 (CD45-)
P2 (CD45+CD11b-SiglecF-)
P3 (CD45+CD11b+SiglecF+ EOS)
Gene/β-actin mRNA fold change
Alox5
Alox12
Alox15
Cox1
Cox2
b)
WT
ΔdblGATA
Merge
c)
WT
ΔdblGATA
ALOX15
β-actin
75 kDa
42 kDa
ALOX15 relative density to β-actin
d)
PC 1
PC 2
PC 3
WT
dblGATA
e)
Type
12-HpETE***
LTD4
PGA2
PGJ2
15-HpETE***
Δ12-PGJ2
15-Deoxy-Δ-12,14-PGJ2
13,14-Dihydro-15-Keto-PGD2
15-Keto-PGF2a
11b-PGF2a
PGD2
14(15)-EET**
17(18)-DiHETE
LTB4
6,15-DiKeto-13,14-Dihydro-PGF1a
11-DehydroTxB2
14(15)-DiHETE*
15-HETE**
13,14-Dihydro-15-Keto-PGE1
8-HETE**
13,14-Dihydro-15-Keto-PGE2*
12-KETE**
12-HETE**
DHA
19(20)-DiHDPA
10-HDHA**
14-HDHA*
17-HDHA***
11-HEPE
PGD3
PGE3
TxB3
Substrate
−3 −2 −1 0 1 2 3
Type
WT
dblGATA
Substrate
AA
DHA
EPA
f)
AA
P450
COX
PGH2
PGD2
PGE2
PGI2
PGF2
13,14-Dihydro-15-Keto-PGE2
14,15-EET
LOX
5-Lox
8-Lox
12-Lox
15-Lox
5-HETE
8-HETE
12-HETE
15-HETE
5-OxoETE
12-OxoETE
15-OxoETE
8,15-DiHETE
LXA4
ND
g)
DHA
20-HDHA
13-HDHA
4-HDHA
7-HDHA
10-HDHA
14-HDHA
17-HDHA
h)
EPA
11,12-DiHETE
18-HEPE
PGH3
5-HEPE
8-HEPE
12-HEPE
15-HEPE
i)
5 nM
10 nM
20 nM
100 nM
Proliferation (% of untreated control)
Untreated
PDGFbb
14-HDHA
17-HDHA
15-HEPE
12-HETE

FIGURE 7 Deficiency of 12/15-lipoxygenase derivatives in lungs of eosinophil (EOS)-deficient (ΔdblGATA) mice. a) Strategy for flow cytometric sorting from lung tissues of C57/BL6 mice (top panel) and relative mRNA expression of *Alox5*, *Alox12*, *Alox15*, *Cox1* and *Cox2* in sorted cells (bottom panel, n=3). b) Representative images of arachidonate 15-lipoxygenase (ALOX15) and SiglecF immunofluorescent staining of lung sections from wild-type (WT) or ΔdblGATA mice. Scale bars: 100 μm (main) and 25 μm (inset). c) Representative Western blots (top panel) and quantification (bottom panel) of ALOX15 in the lungs of WT and ΔdblGATA mice with pulmonary hypertension (PH) (n=6 per group). d) Principal component (PC) analysis of lipidomics data. e) Heatmap showing key lipid derivatives differentially expressed in lung tissues of WT or ΔdblGATA mice with PH (n=9 per group). f) Quantification of arachidonic acid (AA)-derived products in lung tissues of WT and ΔdblGATA mice with PH (n=9 per group). g) Quantification of docosahexaenoic acid (DHA)-derived products in lung tissues of WT and ΔdblGATA mice with PH (n=9 per group). h) Quantification of eicosapentaenoic acid (EPA)-derived products in lung tissues of WT and ΔdblGATA mice with PH (n=9 per group). i) The percentage of mouse pulmonary artery smooth muscle cell (PASMC) proliferation after treatment with platelet-derived growth factor bb (PDGFbb) (10 ng·mL^{-1}) and different concentrations of 12/15-LOX derivatives (5 nM, 10 nM, 20 nM, 100 nM) compared with untreated control, measured by Cell Counting Kit-8 (Sigma Aldrich). For a and i, differences between groups were evaluated by one-way ANOVA with Bonferroni's *post hoc* test. For c, f–h, differences were evaluated by unpaired two-tailed t-test. All data are shown as mean±SEM. NS: nonsignificant; ND: not detected. *: p<0.05; **: p<0.01; ***: p<0.001; ****: p<0.0001 for 12/15-LOX derivatives-treated groups *versus* PDGFbb-treated groups, or WT *versus* ΔdblGATA mice with PH. #: p<0.05; ##: p<0.01 for PDGFbb-treated group compared with untreated control group.

Discussion

In this study, we found that EOS migrate from peripheral blood into lung tissue during PH development, and fibroblast-derived CCL11 might be responsible for EOS pulmonary recruitment. Furthermore, EOS deficiency aggravated PH, increased neutrophil and monocyte/macrophage infiltration, and promoted PASMC proliferation. We further demonstrated that EOS function through 12/15-lipoxygenease metabolites, and that downstream 14/17-HDHA mediates anti-inflammatory effects in immune cells through the SPM receptor FPR2, while inhibiting PASMC proliferation through PPARγ activation (figure 8g).

Although the protective effects of EOS have been reported in many diseases, the underlying mechanisms vary [10, 11, 15, 16, 22–24]. In addition to the lipid mediators reported in our study and other studies, EOS granular proteins and cytokines have also been revealed to have protective effects in the progression of various diseases. For example, in myocardial infarction and abdominal aortic aneurysm development, EOS were reported to function through eosinophil-associated ribonuclease-1 (mouse Ear1, a human ECP homologue) and IL4 [10, 11], and through IL13 in liver injury [22]. However, these EOS-derived mediators also exist in other immune cells in lung tissue, suggesting that EOS are not the main source of these compounds: Ear1 is mainly secreted by alveolar macrophages [39, 40] and cytokines such as IL4 and IL13 are mainly derived from Th2 cells and mast cells [2, 3]. By contrast, the 12/15-lipoxygenase metabolites found in our study were uniquely expressed by EOS in lung tissues. EOS depletion largely repressed the production of lipid mediators in the lung, which participate in EOS-mediated PH development.

In our study, we have identified 14-HDHA and 17-HDHA as the downstream lipid mediators produced by 12/15-lipoxygenase. The pro-resolving effect of 14-HDHA and 17-HDHA is well reported. Our study showed 14/17-HDHA suppressed inflammatory cell adhesion and migration through FPR2. Moreover, the scRNA-seq data showed that SPM receptor FPR2 was mainly expressed in neutrophils, macrophages and monocytes, suggesting only these cells were capable of responding to EOS-derived SPM shortage in EOS-deletion mouse lungs. Besides, 14-HDHA and 17-HDHA are also the precursors of SPMs, such as protectins, resolvin and maresins [32]. Although UHPLC-MS/MS showed very low concentrations of these SPMs, we still cannot deny their effective roles in resolving inflammation.

Of note, we also showed that 14-HDHA and 17-HDHA exhibited an anti-proliferative effect on PDGFbb-induced PASMCs. 14-HDHA and 17-HDHA are lipid metabolites oxidised from docosahexaenoic acid. Lipid metabolites serve as the ligand of PPARγ [41]. These lipid ligands promoted PPARγ forming a heterodimer with retinoid X receptor, and subsequently binding to the peroxisome proliferator response element gene promoter [41]. This process has been documented for years, but mostly in metabolic syndromes [42]. In our study, we found that 14-HDHA and 17-HDHA promoted PPARγ activation and nuclear translocation in PASMCs. In PASMCs, activated PPARγ bound to Stat3 and inhibited Stat3 shuttling [36]. The same result could also be observed in 14/17-HDHA-activated PASMCs. 14/17-HDHA stimulation promotes PPARγ and blunts Stat3 phosphorylation, resulting in maintenance of PASMC homeostasis.

In the current study, we found low levels of EOS in the peripheral blood of PAH patients and SuHx-induced PH mice and rats compared with control subjects/animals. This could be due to increased

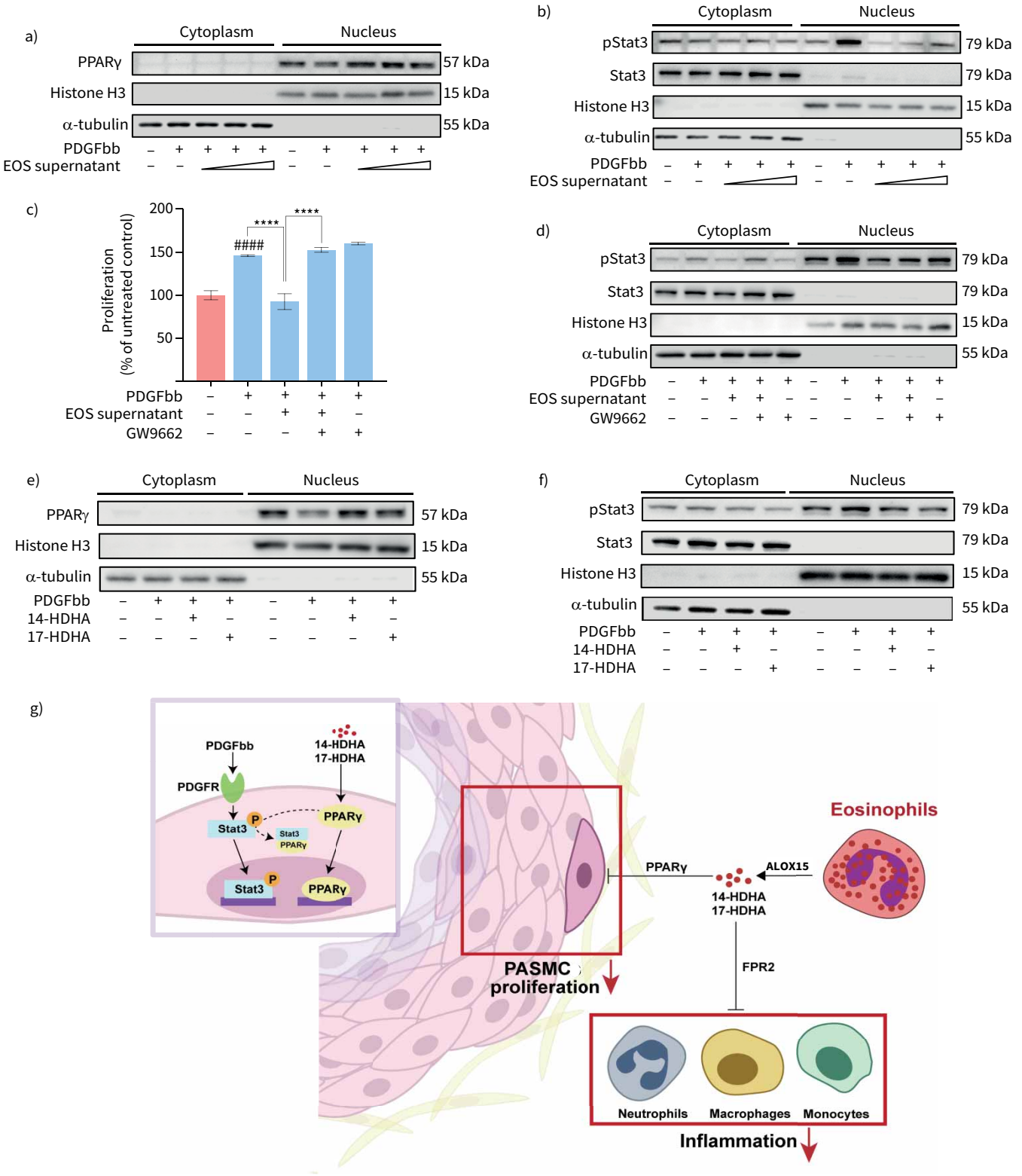

FIGURE 8 Eosinophil (EOS)-derived 14/17-HDHA inhibits pulmonary artery smooth muscle cell (PASMC) proliferation by activating peroxisome proliferator-activated receptor γ (PPARγ). a) Representative Western blots of PPARγ in cytoplasmic and nuclear extracts of mouse PASMCs treated with platelet-derived growth factor bb (PDGFbb) and different concentrations of EOS supernatant (equivalent to 1×10^4, 1×10^5, 1×10^6 EOS·mL^{-1}) for 24 h (n=3). b) Representative Western blots of Stat3 and phosphorylated Stat3 (pStat3) in cytoplasmic and nuclear extracts of mouse PASMCs treated with PDGFbb (10 ng·mL^{-1}) and different concentrations of EOS supernatant (equivalent to 1×10^4, 1×10^5, 1×10^6 EOS·mL^{-1}) for 24 h (n=3). c) The percentage of mouse PASMC proliferation pre-incubated with GW9662 (1 μM) or dimethyl sulfoxide (DMSO) for 24 h, then treated with

PDGFbb (10 ng·mL^{-1}) and EOS supernatant (equivalent to 1×10^5 EOS·mL^{-1}) for another 24 h compared with untreated control. d) Representative Western blots of Stat3 and pStat3 in cytoplasmic and nuclear extracts of mouse PASMCs pre-incubated with GW9662 or DMSO for 24 h, then treated with PDGFbb and EOS supernatant (equivalent to 1×10^5 EOS·mL^{-1}) for another 24 h (n=3). e) Representative Western blots of PPARγ in cytoplasmic and nuclear extracts of mouse PASMCs treated with PDGFbb and 14-HDHA or 17-HDHA (10 nM) for 24 h (n=3). f) Representative Western blots of Stat3 and pStat3 in cytoplasmic and nuclear extracts of mouse PASMCs treated with PDGFbb and 14-HDHA or 17-HDHA (10 nM) for 24 h (n=3). g) Schematic representation of the proposed mechanism underlying EOS-mediated protection in pulmonary hypertension. For c, differences between groups were evaluated by one-way ANOVA with Bonferroni's *post hoc* test. ALOX15: arachidonate 15-lipoxygenase; FPR2: N-formyl peptide receptor 2. ****: p<0.0001 for other groups *versus* EOS supernatant-treated groups; ####: p<0.0001 for PDGFbb-treated group compared with untreated control group.

EOS migration to the lungs but no significant change in EOS generation in bone marrow. Thus, EOS maintained tissue homeostasis and played a protective role in the lung. However, detrimental effects with high levels of EOS have been reported in pulmonary inflammation mouse models induced by ovalbumin (OVA) sensitisation/challenge [43] or long-term IL33 treatment [44]. Apparently, there are functional differences between the low and high EOS conditions, which might be due to the different EOS subtypes. Previous studies have reported two EOS subtypes in lung tissue classified by CD101 expression: CD101$^-$ resident EOS and CD101$^+$ inflammatory EOS [20]. CD101$^-$ resident EOS were present in steady states, while CD101$^+$ inflammatory EOS were differentiated when receiving antigen stimulation (such as house dust mites or OVA) [15, 20]. In our study, there were no exogenous antigens applied in animal models and allergic diseases were excluded in enrolled human samples. We found no aberrant EOS generation in bone marrow, and CD101$^-$ resident EOS were the major functional subtype in bone marrow, blood and lungs. These resident EOS play a protective role in PH development. However, in those animal models with eosinophilia (high EOS levels), exogenous antigens or recombinant cytokines were used, which might affect EOS lineage maturation and differentiation. It warrants further investigation whether more EOS generation leads to eosinophilia and whether inflammatory EOS participate in disease development upon antigen stimulation. The fact that resident EOS and inflammatory EOS are two subtypes with different functions may explain the functional differences between low and high EOS conditions. Of note, eosinophilia can also be observed in patients with chronic obstructive pulmonary disease (COPD). Patients with eosinophilic COPD have a higher risk of PH onset [45]. Therefore, distinguishing the subtypes and specific functions of EOS between PAH patients (without allergic history) and COPD-PH patients (with eosinophilia) would help to comprehensively reveal the function of EOS in different types of PH.

The different EOS subtypes could also explain their different functions in PH and asthma. PAH and asthma share many pathophysiogical features, such as inflammation, vascular reactivity and structural remodelling [46]. EOS aggravate tissue damage in asthma [12], whereas they play a protective role in PAH. A previous study reported that inflammatory EOS are the predominant subtype in an OVA-induced asthma mouse model [20], while in PH we revealed that EOS that have infiltrated into lungs are mainly resident EOS (supplementary figure S1). Therefore, although similar, the pathophysiological heterogeneity of EOS needs to be evaluated in detail.

In PH development, EOS infiltration was also found in the right ventricle of PH mice (figure 2h). Right ventricular hypertrophy and impairment also occurred in PH development; however, the role of EOS in right ventricular hypertrophy remains unclear. A previous study reported the involvement of EOS in left ventricular function [11]. EOS protect cardiac function after acute myocardial infarction through a decrease in cardiomyocyte death, cardiac fibrosis and neutrophil adhesion [11]. Therefore, we speculate that EOS exhibit a similar function in the right ventricle, which should be investigated experimentally in the future.

Despite focusing on EOS in the current animal study, we do not exclude the possibility that other myeloid cells and cytokine signalling pathways may be involved. For example, aberrant basophil lineage maturation was observed in a transgenic mouse line with EOS lineage ablation produced by genetically deleting the GATA1 promoter, which is because GATA1 controls not only EOS but also other myeloid cells, such as basophils [47]. Thus, the effects observed in ΔdblGATA mice may be partially caused by basophil loss. Besides, in TRFK5-treated mice, neutralising IL5 arrested EOS maturation. However, IL5 is not the only ligand for its receptor IL5 receptor α (IL5Rα) (the β common cytokine receptor), IL3 and granulocyte–macrophage-colony stimulating factor (GM-CSF) also share the β common cytokine receptor [48, 49]. Thus, neutralising IL5 might free IL5Rα from IL5 binding and subsequently enhance the signalling for IL3 and GM-CSF binding. GM-CSF and IL3 exhibit strong abilities in activating JAK/STAT signalling and regulating chronic inflammation [49, 50]. Therefore, the observations in TRFK5-treated mice could be

partially induced by GM-CSF and IL3. Nevertheless, when using two different animal models (transgenic EOS deletion and pharmaceutical EOS depletion), we observed consistent results in mice and rats, suggesting the protective role of EOS in PH development. Further study with transgenic eosinophil-deficient mice (PHIL mice) or mice treated with a neutralising antibody against IL5Rα would provide more comprehensive evidence for our conclusions.

Taken together, we found that decreasing EOS with neutralising IL5 subsequently aggravated PH development *via* 14/17-HDHA in animal models. Our study provides proof-of-concept that clinical use of an anti-IL5 monoclonal antibody (such as mepolizumab) might increase the risk of PH onset in patients. The mechanism (EOS–14/17-HDHA–FPR2/PPARγ axis) revealed in our study may suggest some other strategies in PAH treatment. For example, exogenous supplement *via* food intake may compensate for a 14/17-HDHA shortage in lung. Alternatively, targeting the downstream effector cells (such as neutrophils, monocytes and smooth muscle cells) could mimic 14/17-HDHA function, similar to activating FPR2 with Ac2-26 and PPARγ with rosiglitazone together to promote the resolution of inflammation and suppress the proliferation of PASMC in lung.

Author contributions: T. Shu: investigation, methodology, visualisation, writing – original draft. J. Zhang: investigation, methodology, visualisation, writing – original draft. Y. Zhou: software, formal analysis, data curation, visualisation. Z. Chen: supervision, writing – review and editing. J. Li: investigation, validation, visualisation. Q. Tang: validation, visualisation. W. Lei: validation. Y. Xing: conceptualisation, supervision, writing – review and editing, project administration. J. Wang: conceptualisation, supervision, writing – review and editing, project administration, funding acquisition. C. Wang: conceptualisation, supervision, project administration, funding acquisition.

Conflict of interest: No competing interests to declare.

Sources of funding: This work was supported by the by CAMS Innovation Fund for Medical Sciences (2021-I2M-1-049 to J. Wang, 2022-I2M-JB-007 to C. Wang, 2021-I2M-1-005 to Y. Xing, 2021-I2M-1-023 to T. Shu), Beijing Natural Science Foundation (Z220019 to J. Wang), Haihe Laboratory of Cell Ecosystem Innovation Fund (HH22KYZX0010 to J. Wang), the National Key Research and Development Program of China (2019YFA0802600 to J. Wang), the National Natural Science Foundation of China (81901588 to Y. Xing), the Non-profit Central Research Institute Fund of Chinese Academy of Medical Sciences (2019JB310001 and 2018JB31001 to C. Wang), State Key Laboratory Special Fund (2060204 to C. Wang) and the Fundamental Research Funds for the Central Universities (3332022141 to J. Zhang). Funding information for this article has been deposited with the Crossref Funder Registry.

References

1 Humbert M, Guignabert C, Bonnet S, *et al.* Pathology and pathobiology of pulmonary hypertension: state of the art and research perspectives. *Eur Respir J* 2019; 53: 1801887.
2 Daley E, Emson C, Guignabert C, *et al.* Pulmonary arterial remodeling induced by a Th2 immune response. *J Exp Med* 2008; 205: 361–372.
3 Chen G, Zuo S, Tang J, *et al.* Inhibition of CRTH2-mediated Th2 activation attenuates pulmonary hypertension in mice. *J Exp Med* 2018; 215: 2175–2195.
4 Lambrecht BN, Hammad H. The immunology of asthma. *Nat Immunol* 2015; 16: 45–56.
5 Harbaum L, Baaske KM, Simon M, *et al.* Exploratory analysis of the neutrophil to lymphocyte ratio in patients with pulmonary arterial hypertension. *BMC Pulm Med* 2017; 17: 72.
6 Stone KD, Prussin C, Metcalfe DD. IgE, mast cells, basophils, and eosinophils. *J Allergy Clin Immunol* 2010; 125: Suppl. 2, S73–S80.
7 Grisaru-Tal S, Itan M, Klion AD, *et al.* A new dawn for eosinophils in the tumour microenvironment. *Nat Rev Cancer* 2020; 20: 594–607.
8 Ramirez GA, Yacoub MR, Ripa M, *et al.* Eosinophils from physiology to disease: a comprehensive review. *Biomed Res Int* 2018; 2018: 9095275.
9 Weller PF, Spencer LA. Functions of tissue-resident eosinophils. *Nat Rev Immunol* 2017; 17: 746–760.
10 Liu CL, Liu X, Zhang Y, *et al.* Eosinophils protect mice from angiotensin-II perfusion-induced abdominal aortic aneurysm. *Circ Res* 2021; 128: 188–202.
11 Liu J, Yang C, Liu T, *et al.* Eosinophils improve cardiac function after myocardial infarction. *Nat Commun* 2020; 11: 6396.
12 Lu Y, Huang Y, Li J, *et al.* Eosinophil extracellular traps drive asthma progression through neuro-immune signals. *Nat Cell Biol* 2021; 23: 1060–1072.
13 Marx C, Novotny J, Salbeck D, *et al.* Eosinophil-platelet interactions promote atherosclerosis and stabilize thrombosis with eosinophil extracellular traps. *Blood* 2019; 134: 1859–1872.

14 Choi Y, Le Pham D, Lee DH, *et al.* Biological function of eosinophil extracellular traps in patients with severe eosinophilic asthma. *Exp Mol Med* 2018; 50: 1–8.
15 Zhu C, Weng QY, Zhou LR, *et al.* Homeostatic and early-recruited CD101^{-} eosinophils suppress endotoxin-induced acute lung injury. *Eur Respir J* 2020; 56: 1902354.
16 Masterson JC, McNamee EN, Fillon SA, *et al.* Eosinophil-mediated signalling attenuates inflammatory responses in experimental colitis. *Gut* 2015; 64: 1236–1247.
17 Galdiero MR, Varricchi G, Seaf M, *et al.* Bidirectional mast cell-eosinophil interactions in inflammatory disorders and cancer. *Front Med (Lausanne)* 2017; 4; 103.
18 Wong TW, Doyle AD, Lee JJ, *et al.* Eosinophils regulate peripheral B cell numbers in both mice and humans. *J Immunol* 2014; 192: 3548–3558.
19 Singh G, Brass A, Knight CG, *et al.* Gut eosinophils and their impact on the mucus-resident microbiota. *Immunology* 2019; 158: 194–205.
20 Mesnil C, Raulier S, Paulissen G, *et al.* Lung-resident eosinophils represent a distinct regulatory eosinophil subset. *J Clin Invest* 2016; 126: 3279–3295.
21 Acharya KR, Ackerman SJ. Eosinophil granule proteins: form and function. *J Biol Chem* 2014; 289: 17406–17415.
22 Wang Y, Yang Y, Wang M, *et al.* Eosinophils attenuate hepatic ischemia-reperfusion injury in mice through ST2-dependent IL-13 production. *Sci Transl Med* 2021; 13: eabb6576.
23 Brigger D, Riether C, van Brummelen R, *et al.* Eosinophils regulate adipose tissue inflammation and sustain physical and immunological fitness in old age. *Nat Metab* 2020; 2: 688–702.
24 Wu D, Molofsky AB, Liang HE, *et al.* Eosinophils sustain adipose alternatively activated macrophages associated with glucose homeostasis. *Science* 2011; 332: 243–247.
25 Galie N, Humbert M, Vachiery JL, *et al.* 2015 ESC/ERS guidelines for the diagnosis and treatment of pulmonary hypertension: the Joint Task Force for the Diagnosis and Treatment of Pulmonary Hypertension of the European Society of Cardiology (ESC) and the European Respiratory Society (ERS): Endorsed by: Association for European Paediatric and Congenital Cardiology (AEPC), International Society for Heart and Lung Transplantation (ISHLT). *Eur Heart J* 2016; 37: 67–119.
26 Galie N, McLaughlin VV, Rubin LJ, *et al.* An overview of the 6th World Symposium on Pulmonary Hypertension. *Eur Respir J* 2019; 53: 1802148.
27 Ciuclan L, Bonneau O, Hussey M, *et al.* A novel murine model of severe pulmonary arterial hypertension. *Am J Respir Crit Care Med* 2011; 184: 1171–1182.
28 Garlisi CG, Kung TT, Wang P, *et al.* Effects of chronic anti-interleukin-5 monoclonal antibody treatment in a murine model of pulmonary inflammation. *Am J Respir Cell Mol Biol* 1999; 20: 248–255.
29 Morrell NW, Aldred MA, Chung WK, *et al.* Genetics and genomics of pulmonary arterial hypertension. *Eur Respir J* 2019; 53: 1801899.
30 Ortega HG, Liu MC, Pavord ID, *et al.* Mepolizumab treatment in patients with severe eosinophilic asthma. *N Engl J Med* 2014; 371: 1198–1207.
31 Klion AD, Ackerman SJ, Bochner BS. Contributions of eosinophils to human health and disease. *Annu Rev Pathol* 2020; 15: 179–209.
32 Gabbs M, Leng S, Devassy JG, *et al.* Advances in our understanding of oxylipins derived from dietary PUFAs. *Adv Nutr* 2015; 6: 513–540.
33 Serhan CN. Pro-resolving lipid mediators are leads for resolution physiology. *Nature* 2014; 510: 92–101.
34 Liu GJ, Tao T, Wang H, *et al.* Functions of resolvin D1-ALX/FPR2 receptor interaction in the hemoglobin-induced microglial inflammatory response and neuronal injury. *J Neuroinflammation* 2020; 17: 239.
35 Sun L, Xu YW, Han J, *et al.* 12/15-Lipoxygenase metabolites of arachidonic acid activate PPARγ: a possible neuroprotective effect in ischemic brain. *J Lipid Res* 2015; 56: 502–514.
36 Calvier L, Chouvarine P, Legchenko E, *et al.* PPARγ links BMP2 and TGFβ1 pathways in vascular smooth muscle cells, regulating cell proliferation and glucose metabolism. *Cell Metab* 2017; 25: 1118–1134.
37 Legchenko E, Chouvarine P, Borchert P, *et al.* PPARγ agonist pioglitazone reverses pulmonary hypertension and prevents right heart failure *via* fatty acid oxidation. *Sci Transl Med* 2018; 10: eaao0303.
38 Hennigs JK, Cao A, Li CG, *et al.* PPARγ-p53-mediated vasculoregenerative program to reverse pulmonary hypertension. *Circ Res* 2021; 128: 401–418.
39 Cormier SA, Yuan S, Crosby JR, *et al.* T_H2-mediated pulmonary inflammation leads to the differential expression of ribonuclease genes by alveolar macrophages. *Am J Respir Cell Mol Biol* 2002; 27: 678–687.
40 Luo M, Lai W, He Z, *et al.* Development of an optimized culture system for generating mouse alveolar macrophage-like cells. *J Immunol* 2021; 207: 1683–1693.
41 Marion-Letellier R, Dechelotte P, Iacucci M, *et al.* Dietary modulation of peroxisome proliferator-activated receptor γ. *Gut* 2009; 58: 586–593.
42 Lodhi IJ, Semenkovich CF. Peroxisomes: a nexus for lipid metabolism and cellular signaling. *Cell Metab* 2014; 19: 380–392.

43 Weng M, Baron DM, Bloch KD, *et al.* Eosinophils are necessary for pulmonary arterial remodeling in a mouse model of eosinophilic inflammation-induced pulmonary hypertension. *Am J Physiol Lung Cell Mol Physiol* 2011; 301: L927–L936.

44 Ikutani M, Tsuneyama K, Kawaguchi M, *et al.* Prolonged activation of IL-5-producing ILC2 causes pulmonary arterial hypertrophy. *JCI Insight* 2017; 2: e90721.

45 Alzghoul BN, As Sayaideh M, Moreno BF, *et al.* Pulmonary hypertension in eosinophilic *versus* noneosinophilic COPD. *ERJ Open Res* 2021; 7: 00772-2020.

46 Said SI, Hamidi SA, Gonzalez Bosc L. Asthma and pulmonary arterial hypertension: do they share a key mechanism of pathogenesis? *Eur Respir J* 2010; 35: 730–734.

47 Nei Y, Obata-Ninomiya K, Tsutsui H, *et al.* GATA-1 regulates the generation and function of basophils. *Proc Natl Acad Sci USA* 2013; 110: 18620–18625.

48 Nelson RK, Brickner H, Panwar B, *et al.* Human eosinophils express a distinct gene expression program in response to IL-3 compared with common β-chain cytokines IL-5 and GM-CSF. *J Immunol* 2019; 203: 329–337.

49 Dougan M, Dranoff G, Dougan SK. GM-CSF. IL-3, and IL-5 family of cytokines: regulators of inflammation. *Immunity* 2019; 50: 796–811.

50 Sawada H, Saito T, Nickel NP, *et al.* Reduced BMPR2 expression induces GM-CSF translation and macrophage recruitment in humans and mice to exacerbate pulmonary hypertension. *J Exp Med* 2014; 211: 263–280.